International Journal of GEOMATE, Dec., 2023 Vol.25, Issue 112, pp.64-74
ISSN: 2186-2982 (P), 2186-2990 (O), Japan, DOI: https://doi.org/10.21660/2023.112.4075
Geotechnique, Construction Materials and Environment

STUDY OF LIQUEFACTION POTENTIAL IN TOLL ROAD CONSTRUCTION ON FINE-GRAINED SOIL

Asep Setyobudianto[1], *Fikri Faris[2] and Hary Christady Hardiyatmo[2]

[1] Master Program in Natural Disaster Management Engineering, Department of Civil and Environmental Engineering, Universitas Gadjah Mada, Indonesia;
[2] Department of Civil and Environmental Engineering, Universitas Gadjah Mada, Indonesia

*Corresponding Author, Received: 01 Aug. 2023, Revised: 17 Nov. 2023, Accepted: 30 Nov. 2023

ABSTRACT: Liquefaction is a natural phenomenon indicating the transformation of soil into a liquid state. This condition occurs when saturated sandy soil experiences shaking, causing an increase in pore water pressure and decreasing effective soil stress. This study aims to assess the liquefaction potential in the Solo-Yogyakarta-NYIA Kulonprogo Toll Road. Although several parameters influence the potential of liquefaction, this toll road must be vigilant due to its proximity to seismic sources. Preparing for liquefaction potential is crucial to ensure the stability of structures throughout their service life. This research thoroughly investigated liquefaction potential from the identification to the evaluation stage of 21 boreholes that indicate highly fine-grained soils. The identification stage was conducted through grain size and soil properties analysis. The evaluation stage used the Factor of Safety (FS) with the Simplified Procedure and the Liquefaction Potential Index (LPI). The identification results show that several boreholes have liquefaction grain gradations and soil properties. The evaluation results using Peak Ground Acceleration (PGA) by Kanno Attenuation resulted in three borehole locations with FS < 1. The classification of liquefaction potential in these three boreholes is high and low. The analysis shows that one of the three boreholes has a significantly higher fines content than the others. Further investigation of this uniqueness can be conducted using another method, such as numerical analysis.

Keywords: Toll, Identification, Evaluation, Liquefaction, Kanno

1. INTRODUCTION

The toll road system represents a strategic infrastructure facilitating connectivity, crucial for economic and tourism growth. A notable toll road currently under construction in Indonesia is the Solo-Yogyakarta-New Yogyakarta International Airport (NYIA) Kulonprogo Toll Road, commonly known as the Jogja-Solo Toll Road. Situated on the southern side of Java Island, this toll road is located within an earthquake-prone region due to the active Opak Fault. This strike-slip fault stretches from Yogyakarta to Klaten, indicating a significant role in the 2006 Yogyakarta earthquake [1]. The road segment located in Klaten Regency and within a radius of 10 km from the northern side of the Opak Fault serves as the research location. Previous studies indicate that this radius experiences the most significant ground acceleration [2]. Furthermore, the northern segment's seismic activity potential is higher than the southern segment [3].

With earthquake vulnerability present, the construction of the Jogja – Solo Toll Road must be vigilant against liquefaction potential. This earthquake-induced phenomenon causes the soil to lose its stability. During an earthquake, the pore water pressure within the soil layer increases, resulting in a reduction or even loss of stress between soil particles [4]. The structural consequences caused by liquefaction include the loss of bearing capacity for foundation bridges, the collapse of underpasses, or the settlement or displacement of embankments. Such events lead to losses in the long-term investments made for toll road construction. Moreover, this toll road plays a vital role in connecting the toll road network in the South of Java, including the Semarang Solo Toll Road on the east and the Yogyakarta - Bawen Toll Road on the north. Damage to the toll road due to unanticipated liquefaction potential can disrupt connectivity in this toll road network.

The analysis of liquefaction potential is an initial step in disaster preparedness. While earthquakes undoubtedly trigger liquefaction, various parameters govern this phenomenon. Stable soil with interlocking grains exhibits more excellent resistance to shocks. Conversely, small grain sizes with irregular shapes and poor gradation can elevate the liquefaction potential [5-7]. Soil properties also provide an influence. Research indicates that adding fines content enhances the resistance to liquefaction [8], whereas silty sand with low plasticity may be highly susceptible to liquefaction [9]. Accordingly, more stringent criteria encompassing fine-grained properties and soil plasticity have been established based on factors such as percent finer, Liquid Limit

(LL), moisture content, and Liquid Index (LI) [10,11]. Regardless of how soil characteristics influence liquefaction, the depth of the groundwater table is the most crucial parameter. Sudden excess pore water pressure causes stress loss between soil particles. A shallow groundwater table increases the liquefaction potential, even in silty soils subjected to dynamic compaction [12]. Field measurements reveal that the groundwater level at the research site lies relatively shallow, ranging from 0 to 6 meters [13].

Based on the explanation above, this research aims to analyze the Jogja-Solo Toll Road's liquefaction potential comprehensively. Although it has a relatively shallow groundwater table, other investigations indicate that the research location contains highly fine-grained soil. This condition implies the importance of a rigorous examination concerning the soil criteria for liquefaction susceptibility. Therefore, the analysis is conducted in two stages, i.e., identification and evaluation. The identification stage is performed to obtain soil layers that exhibit liquefaction behavior during an earthquake. After obtaining these layers, the evaluation stage is conducted to determine the safety factor and liquefaction potential index. Grain gradation and soil properties criteria constrain the identification stage, while the evaluation stage is limited by calculations based on the Standard Penetration Test (SPT). The identification and evaluation stages sequence is expected to produce reliable outputs, which can be followed by liquefaction mitigation for toll road construction.

2. RESEARCH SIGNIFICANCE

This research significantly enhances the management of natural disasters in national strategic projects. Revealing borehole locations with liquefaction potential offers crucial insights for government and construction companies in determining liquefaction mitigation. Moreover, the research has valuable implications for spatial planning policies. Permits for residential and high-risk industrial areas need to exercise caution in proximity to areas with liquefaction potential. Such policies represent the initial step in preventing casualties resulting from liquefaction. Deterministic Peak Ground Acceleration (PGA) also yields reliable values for areas near the earthquake source, providing effective outcomes in addressing seismic hazards of toll road constructions.

3. MATERIALS AND METHODS

The research was conducted in Section 1.2, STA 22+475 – STA 29+000. This segment traverses four sub-districts: Ngawen, Karangnongko, Kebonarum, and Jogonalan, all situated in Klaten Regency, Central Java Province. Figure 1 provides an overview of the research location and the distribution of boreholes designated as locations for the Standard Penetration Test (SPT). The SPT assesses soil penetration by recording the number of

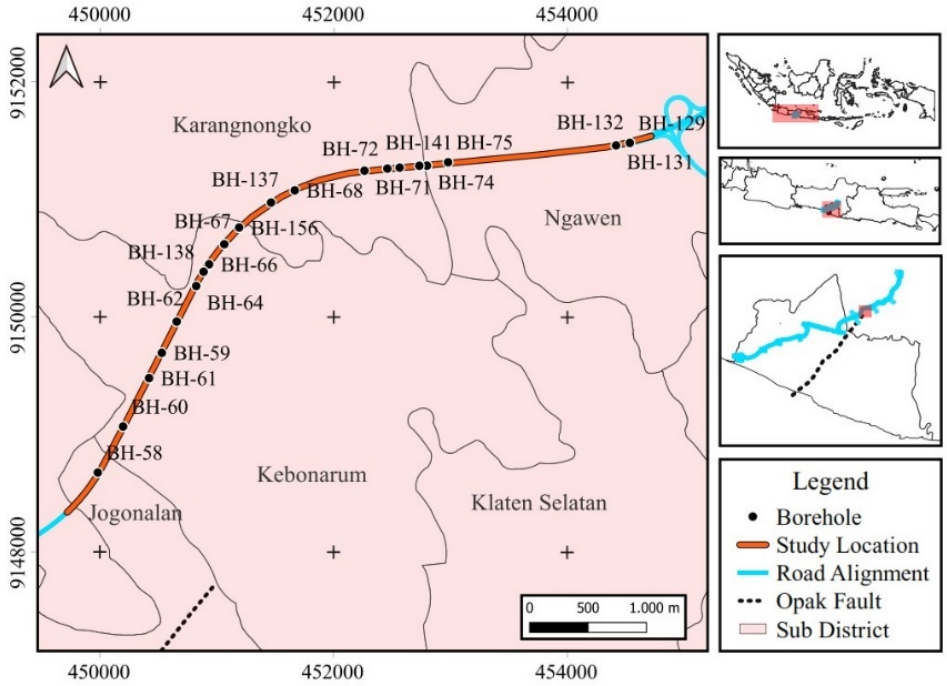

Fig. 1 Distribution of boreholes in toll road segment. The dashed black line depicts the trace of the Opak Fault, situated within a distance of less than 10 km from the research location.

blows from a weighted hammer dropped from a height of 76 cm to drive the sampler to a depth of 15 cm [9]. In this study, 21 boreholes were utilized, with the number of blows recorded at every 2-meter depth. The advantage of the SPT lies in its provision of sand samples, facilitating the determination of fine grains and other grain characteristics [14]. In this research, all SPT and laboratory results were obtained from Jogjasolo Marga Makmur Corporation (JMM), investor and operator of the toll road.

As mentioned, identifying soil layers with liquefaction potential involves two main stages. The first stage entails identification based on grain gradation and soil properties, with only soil layers meeting specific criteria progressing to the subsequent evaluation stage. In the evaluation stage, the Factor of Safety (FS) and the Liquefaction Potential Index (LPI) are calculated to determine the potential of soil that meets liquefaction criteria during an earthquake. The criteria and methods used are explained as follows:

3.1 Identification of Liquefaction Potential

3.1.1 Grain Gradation Criteria

This initial stage begins with plotting the grain size distribution of soil samples on the Tsuchida curve [15]. This curve considers limitations related to the diameter, the proportion of liquefiable grains, and factors such as silt content and a small amount of gravel commonly found in sandy soil layers.

3.1.2 Soil Properties Criteria

While it is widely acknowledged that sandy soil layers predominantly experience liquefaction, it is essential to recognize that under specific criteria, fine-grained soils can also be susceptible to liquefaction. This study adopts the criteria proposed by [10-11], encompassing the following conditions: (1) granules smaller than 0.005 mm ≤ 15%, (2) Liquid Limit (LL) < 35%, (3) water content (w) ≥ 0.9LL, and (4) Liquid Index (LI) ≤ 0.75. Only soil layers satisfying all four criteria are deemed to possess liquefaction potential when subjected to seismic shocks.

3.2 Evaluation of Liquefaction Potential

3.2.1 Determination of (PGA)

The earthquake source used in this research was the May 27, 2006, Yogyakarta earthquake, with a magnitude of 6.3 Mw at coordinates 7.955^0S and 110.430^0E and a depth of 10 km [16]. This record calculates PGA, the maximum ground motion due to an earthquake. PGA causes saturated undrained soil to undergo compression and increases pore water pressure. This research calculates PGA deterministically using the Kanno attenuation [17]. Many earthquake records were used in formulating this attenuation, precisely 96,698 records from within and outside Japan. The model employed is simple, involving only three variables: earthquake magnitude, source distance, and focal depth. Based on previous studies, this attenuation provides the best level of reliability compared to some other attenuators [18]. The Kanno attenuation, consistent with this study, is shown in eq. 1:

$$\log pre = a_1 M_w + b_1 X - \log(X + d_1 . 10^{0,5 M_w}) + c_1 + \varepsilon_1 \ (D \leq 30\ km) \quad (1)$$

Here, *Pre* is the predicted PGA (cm/sec^2), Mw is the moment magnitude (M_w), X is the source distance (km), and D is the focal depth (km). Table 1 shows a_1, b_1, c_1 , d_1 as the regression coefficient and ε_1 as the error between observed and predicted values:

Table 1 Regression coefficient and error value [17]

a_1	b_1	c_1	d_1	ε_1
0.56	-0.0031	0.26	0.0055	0.37

As shown in eq. 2, Kanno provides correction values to improve prediction results based on site effects correction.

$$G = \log(obs/pre) = p \log AVS30 + q \quad (2)$$

Here, G is the site effect correction (cm/s^2), AVS30 is the average of shear wave velocity (m/s), and p and q are regression coefficients of -0,55 and 1,35 (for PGA). The predicted PGA after applying the site effect correction is calculated by eq. 3:

$$\log pre_G = \log pre + G \quad (3)$$

Another correction proposed by Kanno is the influence of the abnormal seismic intensity on the Pacific Plate in North Japan caused by medium and deep earthquakes. This correction is not used in this study because the earthquake source is shallow earthquakes affected by fault movements.

3.2.2 Determination of VS30

The AVS30 value in eq. 2 is derived from the average shear wave velocity at 30-meter depth (VS30). This value is calculated by the correlation proposed by [19] with eq. 4.

$$Vs = 119 SPT^{0,2051} \quad (4)$$

Here, Vs is the shear wave velocity (m/s), and SPT is the value of the Standard Penetration Test. This approach was selected by considering that the calculation of RMSE (Root Mean Square Error) from this correlation produces the slightest error compared to 18 previous studies, resulting in the

lowest deviation and modeling the observation data adequately [19].

3.2.3 Factor of Safety

The Factor of Safety (FS) is determined by the Simplified Procedure based on SPT [20]. Several parameters are corrected as an adjustment of site characteristics to the liquefaction record that forms this procedure, i.e., Magnitude Scaling Factor (MSF), shear stress reduction (r_d), SPT blow count corrected to energy, overburden stress, and equivalent clean sand ($(N_1)_{60cs}$) [21]. The boreholes with liquefaction potential are determined by FS < 1, calculated by eq. 5.

$$FS = \frac{CRR_{M,\sigma'_{vc}}}{CSR_{M,\sigma'_{vc}}} \quad (5)$$

Here, $CRR_{M,\sigma'_{vc}}$ is the Cyclic Resistance Ratio of actual magnitude and effective vertical stress, $CSR_{M,\sigma'_{vc}}$ is the Cyclic Stress Ratio of actual magnitude and effective vertical stress. $CRR_{M,\sigma'_{vc}}$ is calculated by eq. 6:

$$CRR_{M,\sigma'_{vc}} = CRR_{M=7,5,\sigma'_{vc}=1atm}.MSF.K_\sigma \quad (6)$$

Here, $CRR_{M=7,5,\sigma'_{vc}=1atm}$ is the CRR at 7,5 Mw and effective vertical stress of 1 atm, requiring correction of Magnitude Scaling Factor (MSF) and an effective overburden pressure (K_σ). MSF is calculated based on MSF_{max} (eq. 7 and eq. 8) which is an update of the previous MSF equation [22].

$$MSF_{max} = 1{,}09 + \left(\frac{(N1)_{60\,cs}}{31{,}5}\right)^2 \leq 2{,}2 \quad (7)$$

$$MSF = 1 + (MSF_{max} - 1)(8.64exp\left(\frac{-M}{4}\right) - 1.325) \quad (8)$$

Here, M is the moment magnitude, $(N_1)_{60\,cs}$ is the corrected penetration resistance $(N_1)_{60}$ equivalent clean sand. This variable is also used in calculating. $CRR_{M=7,5,\sigma'_{vc}=1atm}$ in eq. 9.

$$CRR_{M=7,5,\sigma'_{vc}=1atm} = \exp\left(\frac{(N1)_{60cs}}{14{,}1} + \left(\frac{(N1)_{60cs}}{126}\right)^2 - \left(\frac{(N1)_{60cs}}{23{,}6}\right)^3 + \left(\frac{(N1)_{60cs}}{25{,}4}\right)^4 - 2{,}8\right) \quad (9)$$

The evaluation continues by determining the CSR value of the stress in the soil when subjected to cyclic loads. The CSR calculation developed by [23] is shown in eq. 10:

$$CSR_{M,\sigma'_{vc}} = 0{,}65.\frac{\sigma_{vc}}{\sigma'_{vc}}.\frac{a_{max}}{g}.r_d \quad (10)$$

Here, σ_{vc} is the total vertical stress (kN/m^2), σ'_{vc} is the effective vertical stress (kN/m^2), a_{max} is the maximum ground acceleration (PGA), g is the gravitational acceleration (9,81 m/s^2), r_d is the shear stress reduction that is affected by the soil.

3.2.4 Liquefaction Potential Index (LPI)

FS only indicates whether a location has liquefaction potential or not. The Liquefaction Potential Index (LPI) can provide the level of damage on the surface related to the FS at deeper soil layers [24]. In addition to FS, the level of surface damage is also considered based on the thickness and depth of the liquefied layer. The LPI is calculated using the equation developed by [25], as shown in equation 11:

$$LPI = \int_0^{20} F(z)w(z)dz \quad (11)$$

Here, z is the depth of the soil layer (m) with w(z)=10-0.5z for z ≤ 20 meters and w(z)=0 for z > 20 meters. Equation (11) is modified by changing the constraints F(z) = 0 for $\boldsymbol{F_L} \geq 1{,}2$; F(z) = 1-$\boldsymbol{F_L}$ for $\boldsymbol{F_L} \leq 0{,}95$; and F(z) = $\mathbf{2.10^6.e^{-18.427(F_L)}}$ for 0,95 < $\boldsymbol{F_L}$ < 1,2 [26]. This modification results in a classification shown in Table 2.

Table 2 Classification of surface damage [26]

LPI	Classification
0	Non liquefied
0 < *LPI* ≤ 2	Low
2 < *LPI* ≤ 5	Moderate
5 < *LPI* ≤ 15	High
LPI > 15	Very High

4. RESULTS AND DISCUSSION

Grain size analysis by the Tsuchida curve shows that BH-64 and BH-71 do not exhibit liquefied grains. All grain samples from these boreholes intersect the boundary curve. An example of the grain gradation analysis is presented in Fig. 2 for BH-67. This borehole has soil layers with grain gradations that meet liquefaction and non-liquefaction criteria. The space between curve 1 indicates the most liquefiable soil, while the space between curve 2 indicates potentially liquefiable soil. Soil samples at 14 and 24 meters depths at curves 1 and 2 boundaries indicate liquefied grain gradation. The curve that is getting straight up shows more uniform gradation than others. This poor gradation increases the liquefaction potential. In contrast to the soil sample at a depth of 3, 9, 19, and 19 meters, the curve intersects with curve 2, showing non-uniform gradations and more resistance to the liquefaction potential. The intersection also describes that this gradation has a relatively high fines content (FC). For clarity, Table 3 shows FC at each borehole.

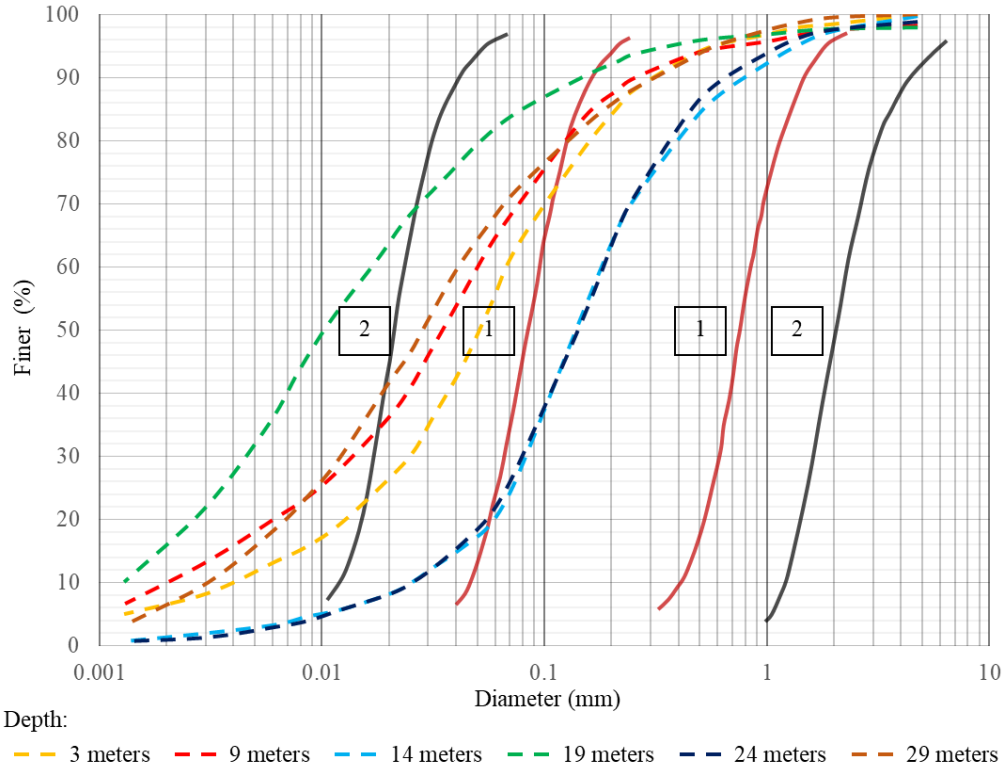

Fig. 2 Grain size on BH-67 (modified from [15]). Soil samples at 14 and 24 meters depth meet the grain criteria. Other samples that intersect curve 2 indicate high fine-grain soil.

Table 3 Fines content at each borehole

D	Borehole Numbers																				
(m)	58	60	61	59	62	64	138	66	67	156	137	68	71	72	155	141	74	75	132	131	129
2	94	89	97	88	84	76	69	88	63	78	34	31	68	86	97	88	95	95	91	92	90
4	94	89	97	88	84	76	69	88	63	78	34	31	68	86	97	88	95	95	91	92	90
6	89	28	97	30	81	74	68	88	70	20	36	75	68	77	81	88	90	94	92	95	69
8	89	28	97	30	81	74	68	88	70	20	36	75	66	77	81	88	90	94	92	95	69
10	77	28	85	92	34	81	68	83	70	20	98	75	66	88	94	96	81	94	81	40	65
12	77	33	85	92	34	81	69	83	26	19	98	43	72	88	94	96	81	93	81	40	65
14	77	33	85	92	34	81	69	83	26	19	21	43	72	88	94	96	81	93	81	40	65
16	22	29	95	20	67	81	69	84	26	19	21	18	72	94	19	82	29	67	64	97	68
18	22	29	95	20	67	81	71	84	85	75	21	18	64	94	19	82	29	67	64	97	68
20	59	29	25	90	38	81	71	32	85	75	20	18	64	94	26	26	29	27	48	98	66
22	59	20	25	90	38	81	70	32	28	18	20	18	74	94	26	26	29	27	48	98	66
24	59	20	25	90	38	81	70	32	28	18	20	■	74	■	26	26	■	29	48	98	66
26	66	19	61	21	40	81	19	21	28	18	19	■	67	■	19	23	■	29	42	24	56
28	66	19	61	21	40	81	19	21	72	80	19	■	67	■	19	23	■	29	42	24	56
30	66	19	61	69	40	81	19	21	72	80	19	■	67	■	19	23	■	29	42	24	56

D = Depth, ■ *= Incomplete data*

Table 3 shows that BH 67 at depths 3, 9, 19, and 29 meters has FC ranging from 63% to 85%. The high fine-grained soil identified from the Tsuchida curve does not fully indicate liquefaction resistance. The ability of soil particles to adhere to each other and maintain a solid form to prevent liquefaction has not been identified. Research by [27] indicates that the plasticity of the soil has a more significant influence on liquefaction potential than its fines-grain gradation, and the use of the Tsuchida curve needs to be restricted to soils with medium to high plasticity. Therefore, the four criteria proposed by [10-11] provide a more detailed identification of liquefaction potential. Table 4 shows an example of the analysis results for BH-67.

Table 4 Identification of fine-grained soils with liquefaction potential in BH-67

D (m)	finner ≤ 5 µm (%)	w (%)	LL	PL	PI	LI	finner ≤ 5 µm ≤ 15%	w ≥ 0.9 LL	LL < 35%	LI ≤ 0.75	Mark
2	13	22	-	NP	-	-	✓	✓	✓	✓	L
4	13	22	-	NP	-	-	✓	✓	✓	✓	L
6	20	26	38	26	13	0.02	x	x	x	✓	NL
8	20	26	38	26	13	0.02	x	x	x	✓	NL
10	20	26	38	26	13	0.02	x	x	x	✓	NL
12	3	22	-	NP	-	-	✓	✓	✓	✓	L
14	3	22	-	NP	-	-	✓	✓	✓	✓	L
16	3	22	-	NP	-	-	✓	✓	✓	✓	L
18	35	47	56	35	22	0.58	x	x	x	✓	NL
20	35	47	56	35	22	0.58	x	x	x	✓	NL
22	2	20	-	NP	-	-	✓	✓	✓	✓	L
24	2	20	-	NP	-	-	✓	✓	✓	✓	L
26	2	20	-	NP	-	-	✓	✓	✓	✓	L
28	18	23	-	NP	-	-	x	✓	✓	✓	NL
30	18	23	-	NP	-	-	x	✓	✓	✓	NL

w = water content, LL = Liquid Limit, PL = Plastic Limit, PI = Plastic Index, LI = Liquid Index, NP = Non Plastic, L = Liquefiable, NL = Not Liquefiable

Table 4 shows layers that only meet the four criteria considered potentially liquefiable (L). An interesting point is illustrated by the soil layer at a depth of 2-4 meters. This layer is considered potentially liquefiable despite having an FC of 63% and not meeting the grain gradation criteria (Fig. 2, 3 meters depth). This is due to the content of particles smaller than 0.005 mm, being only 13%, indicating a prevalence of silt in the fine-grained soil. Additionally, the LL, PI, and LI values cannot be defined (-), suggesting that the soil is non-plastic (NP) based on laboratory tests. The occurrence of NP (non-plastic soil) can be attributed to challenges in conducting the Atterberg test for soil samples, primarily because of the low plasticity nature of the soil. The differences in the results of grain gradation identification with soil properties do not necessarily contradict these two approaches. On the contrary, these two approaches can complement each other, as seen in the grain gradation at 14 and 24 meters depth (Figure 2), where the soil properties are also identified to be liquefied (Table 4). Later, the evaluation stage will more precisely determine soil layers that have the liquefaction potential because the influence of earthquakes and other liquefaction parameters will be considered.

In this research, the identification stage divided soil layers into 3 categories. The first category (NL) indicates layers that do not meet both gradation and soil property criteria. The second category (L) indicates layers that meet both gradation and soil property criteria. The third category (L*) indicates layers that do not meet gradation criteria but meet soil property criteria. Table 5 shows the overall identification results with these three categories.

Table 5 Recapitulation of the borehole that meets the liquefaction criteria

D	Boreholes Numbers																				
(m)	58	60	61	59	62	64	138	66	67	156	137	68	71	72	155	141	74	75	132	131	129
2	NL	NL	NL	NL	NL	NL	NL	NL	L*	NL	L*	L*	NL	NL	NL	NL	NL	NL	NL	NL	NL
4	NL	NL	NL	NL	NL	NL	NL	NL	L*	NL	L*	L*	NL	NL	NL	NL	NL	NL	NL	NL	NL
6	NL	L	NL	L	NL	NL	NL	NL	NL	L	L*	NL	NL	NL	NL	NL	NL	NL	NL	NL	NL
8	NL	L	NL	L	NL	NL	NL	NL	NL	L	L*	NL	NL	NL	NL	NL	NL	NL	NL	NL	NL
10	NL	L	NL	NL	L	NL	NL	NL	NL	L	NL	NL	NL	NL	NL	NL	NL	NL	NL	L*	L*
12	NL	L	NL	NL	L	NL	NL	NL	L	L	NL	L*	NL	NL	NL	NL	NL	NL	NL	L*	L*
14	NL	L	NL	NL	L	NL	NL	NL	L	L	L	L*	NL	NL	NL	NL	NL	NL	NL	L*	L*
16	L	L	NL	L	NL	NL	NL	NL	L	L	L	L	NL	NL	L	NL	L	NL	NL	NL	NL
18	L	L	NL	L	NL	NL	NL	NL	NL	NL	L	L	NL	NL	L	NL	L	NL	NL	NL	NL
20	L*	L	L	NL	L	NL	NL	L	NL	NL	L	L	NL	NL	L	L	L	L	L*	NL	L*
22	L*	L	L	NL	L	NL	NL	L	L	L	L	L	NL	NL	L	L	L	L	L*	NL	L*

Table 5 (Continued) Recapitulation of the borehole that meets the liquefaction criteria

D	Borehole Numbers																				
(m)	58	60	61	59	62	64	138	66	67	156	137	68	71	72	155	141	74	75	132	131	129
24	L*	L	L	NL	L	NL	NL	L	L	L	L		NL		L	L		L	L*	NL	L*
26	L*	L	L*	L	L	NL	L	L	L	L	L		NL		L	L		L	L	L	L*
28	L*	L	L*	L	L	NL	L	L	NL	NL	L		NL		L	L		L	L	L	L*
30	L*	L	L*	L	L	NL	L	L	NL	NL	L		NL		L	L		L	L	L	L*

The identification stage produces soil layers with liquefaction potential marked as "L" and "L*" as shown in Table 5. Both of these categories are used in the evaluation stage because their particles are susceptible to liquefaction during an earthquake, including for high-fine-grained soils with low plasticity that do not meet gradation criteria. In the evaluation stage, potentially liquefiable soil layers are determined by analyzing the Factor of Safety based on the Simplified Procedure. The groundwater level becomes crucial before calculations because liquefaction only occurs when the soil is water-saturated. From the groundwater level in Figure 3, the calculation of the liquefaction potential at BH-67 starts from a depth of 2 meters.

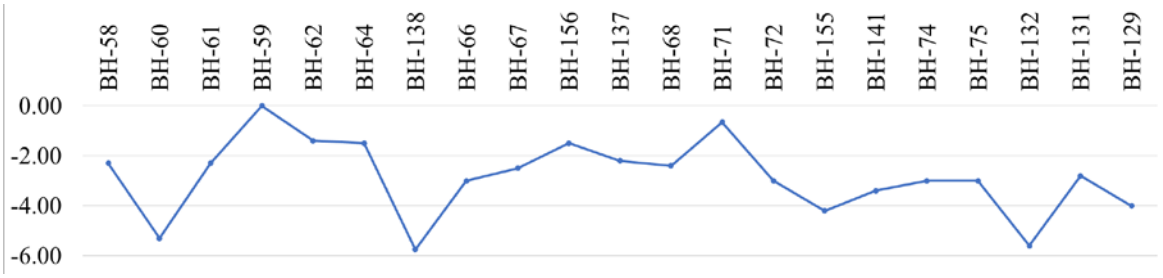

Fig. 3 Groundwater level at each borehole

Another critical parameter is PGA. Table 6 shows the results of PGA calculated by Kanno attenuation. Correction of site effects adds little predictive value, around log 0.02 – log 0.06, resulting in a predicted PGA between 0.27 g - 0.32 g. The comparison of PGA with different methods indicates compliance with Kanno's attenuation. Research by [28] showed that PGA with a 475-year return period in Klaten Regency was 0.21 g - 0.25 g. This value is on bedrock (VS30 = 760 m/s). Considering an amplification factor of 1.39 for 0.21 g and 1.35 for 0.25 g, PGA at the ground surface yields a range of 0.29 g to 0.34 g. This result closely aligns with the PGA value obtained in this research. The amplification factor is derived from [29] for the medium soil class (SD), as classified by the results of AVS30 correlation (Table 6). The conformity of PGA results was also found in [30]. The research estimated PGA based on The Modified Mercalli Intensity of the 2006 Yogyakarta Earthquake. The results indicate that the north zone of the Opak Fault has PGA with an upper limit of 0.3 g. Both conformities suggest that using Kanno's attenuation sufficiently represents seismic hazard based on the earthquake history. In addition to its compatibility with previous research, Kanno's attenuation uses the distance variable from the earthquake source, resulting in a specific PGA at each borehole to evaluate the Factor of Safety (FS).

Table 6 Result of PGA

BH	X (km)	AVS30 (m/s)	PGA (g)
58	32.42	247.83	0.31
60	32.84	237.72	0.32
61	33.29	242.72	0.31
59	33.52	240.24	0.31
62	33.80	232.24	0.31
64	34.13	239.95	0.30
138	34.26	231.40	0.31
66	34.33	227.94	0.31
67	34.54	221.31	0.31
156	34.71	234.34	0.30
137	35.01	260.66	0.28
68	35.18	245.66	0.29
71	35.57	249.11	0.28
72	35.67	228.62	0.30
155	35.73	225.51	0.30
141	35.81	230.67	0.29
74	35.84	256.42	0.28
75	35.95	231.30	0.29
132	36.72	232.11	0.28
131	36.72	227.21	0.29
129	36.80	249.42	0.27

PGA affects CSR, the stress due to cyclic loads that CRR will withstand. If CSR is more excellent than CSR, the FS will be less than 1, which means the soil layer has a liquefaction potential during the

earthquake. Table 7 shows an example of FS calculating at BH 67. The results shows FS < 1 only occurring at a depth of 4 meters. Interestingly, this layer consists of high fine-grained that does not meet the gradation criteria. Other variables influence, especially the lowest of $(N_1)_{60cs}$ at 4 meters depth compared to other layers. Some layers with FS = n.a indicate that these layers were not evaluated because the soil identification did not meet the liquefaction criteria. The overall results of FS are presented in Table 8.

Table 7 Factor of Safety at BH-67

D (m)	$(N_1)_{60cs}$	MSF	Kσ	CRR	CSR	FS
2	-	-	-	-	-	-
4	8.21	1.07	1.05	0.12	0.26	0.47

Table 7 (Continued) Factor of Safety at BH-67

Depth (m)	$(N_1)_{60cs}$	MSF	Kσ	CRR	CSR	FS
6	11.26	1.10	1.03	0.14	0.28	n.a
8	10.68	1.09	1.00	0.14	0.28	n.a
10	29.84	1.46	0.97	0.67	0.28	n.a
12	32.73	1.54	0.93	1.04	0.27	3.87
14	37.32	1.56	0.87	2.58	0.26	9.96
16	27.86	1.40	0.90	0.47	0.25	1.93
18	32.44	1.53	0.86	0.90	0.24	n.a
20	24.47	1.32	0.89	0.32	0.23	n.a
22	46.02	1.56	0.76	2.38	0.22	10.91
24	43.60	1.56	0.74	2.29	0.21	11.04
26	35.93	1.56	0.73	1.54	0.20	7.73
28	42.27	1.56	0.69	2.16	0.19	n.a
30	41.68	1.56	0.67	2.10	0.19	n.a

Table 8 Results of the Factor of Safety

D	Borehole Numbers																				
(m)	58	60	61	59	62	64	138	66	67	156	137	68	71	72	155	141	74	75	132	131	129
2	-	-	-	n.a	n.a	n.a	-	-	-	n.a	-	-	n.a	-	-	-	-	-	-	-	-
4	n.a	-	n.a	n.a	n.a	n.a	-	n.a	0.5	n.a	14.8	1.0	n.a	n.a	-	n.a	n.a	n.a	-	n.a	-
6	n.a	1.3	n.a	8.9	n.a	n.a	n.a	n.a	n.a	8.6	13.5	n.a	n.a	n.a	n.a	n.a	n.a	n.a	n.a	n.a	n.a
8	n.a	12.6	n.a	9.6	n.a	n.a	n.a	n.a	n.a	9.5	12.4	n.a	n.a	n.a	n.a	n.a	n.a	n.a	n.a	n.a	n.a
10	n.a	0.6	n.a	n.a	2.0	n.a	n.a	n.a	n.a	3.5	n.a	n.a	n.a	n.a	n.a	n.a	n.a	n.a	n.a	1.1	13.7
12	n.a	2.1	n.a	n.a	2.2	n.a	2.7	n.a	3.9	0.9	n.a	11.3	n.a	n.a	n.a	n.a	n.a	n.a	n.a	11.0	13.1
14	n.a	0.7	n.a	n.a	9.6	n.a	1.6	n.a	10.0	2.7	11.5	11.3	n.a	n.a	n.a	n.a	n.a	n.a	n.a	11.0	12.9
16	10.4	0.5	n.a	1.1	9.0	n.a	1.5	n.a	1.9	1.0	11.6	11.4	n.a	n.a	3.9	n.a	11.6	1.1	12.3	n.a	n.a
18	2.1	11.1	n.a	3.9	4.6	n.a	n.a	n.a	n.a	n.a	11.7	11.5	n.a	n.a	1.8	n.a	11.8	1.8	6.2	n.a	n.a
20	7.1	9.4	10.7	n.a	9.8	n.a	n.a	10.7	n.a	n.a	5.2	11.7	n.a	n.a	1.9	1.6	12.0	2.4	12.4	n.a	12.9
22	10.8	11.3	10.9	n.a	10.4	n.a	n.a	10.9	10.9	5.2	1.9	11.8	n.a	n.a	8.0	2.1	12.2	1.8	12.5	n.a	13.0
24	11.0	7.4	11.1	n.a	10.6	n.a	n.a	11.1	11.0	2.7	2.3		n.a		12.1	11.7		7.5	3.0	n.a	13.1
26	11.0	11.4	11.2	10.7	10.7	n.a	3.3	5.9	7.7	5.3	1.3		n.a		5.0	11.8		7.5	3.5	1.6	4.8
28	11.1	8.9	11.2	10.8	10.8	n.a	4.1	4.4	11.2	5.8	3.6		n.a		12.1	11.8		11.9	6.6	11.8	3.8
30	11.0	9.8	11.2	10.8	10.8	n.a	4.7	4.9	11.1	7.7	7.4		n.a		10.3	11.8		9.6	3.3	11.8	6.0

Table 8 shows BH-60, BH-67, and BH-156, that in Kebonarum Sub-District (Fig. 1) have FS < 1. The evaluation of FS is the final process of determining whether a borehole has liquefaction potential or not because its calculation involves earthquake potential, depth, soil strength, and stress (eq.5 – eq.10). Compared with the FC value (Table 3), BH-67 has the highest FC (63%). This value is much greater than BH-60 (28%-33%) and BH-156 (19%), showing that soil layers with high FC can also liquefy. However, this condition remains unique because other layers with FC < 63% lack liquefaction potential. This difference could be influenced by the minimal SPT values at BH-67, considering that this parameter affects $(N_1)_{60cs}$ in determining CRR (eq. 9). To enhance the analysis of liquefaction potential in high fine-grained soil, the use of numerical methods can be considered. Research by [9] states that the Simplified Procedure is more appropriate for sand with low fines content, while the behavior of sand during earthquakes is a complex phenomenon influenced by confinement pressure and initial voids ratio. Both parameters can be modeled using a numerical approach to analyze liquefaction potential more realistically in high fine-grained soil with low plasticity.

The evaluation stage is continued by determining the Liquefaction Potential Index (LPI). This stage is crucial because the Factor of Safety evaluation only indicates the presence or absence of liquefaction potential in each layer. The severity level at the surface has not been directly indicated based on the FS value. However, liquefied layers could be distributed over a certain thickness and depth. Table 9 shows the calculation of the LPI. F(z) represents the severity level influenced by the Factor of Safety (FS), while w(z) is the depth factor of the layer. LPI is obtained through the F(z), w(z),

and the thickness of the liquefied layer. The total index in Table 9 shows that BH-60 and BH-67 have a high liquefaction potential, while BH-156 has a low liquefaction potential. The total index determines the level of surface damage due to liquefaction (Table 2). This means that BH-60 and BH-67 have a high level of damage due to liquefaction, whereas BH-156 has a low level of damage.

Table 9 Results of the LPI

Depth	BH-60				BH-67				BH-156			
(m)	FS	F(z)	w(z)	LPI	FS	F(z)	w(z)	LPI	FS	F(z)	w(z)	LPI
2	-	-	-	-	-	-	-	-	n.a	0.00	9.00	0.00
4	-	-	-	-	0.47	0.53	8.00	8.54	n.a	0.00	8.00	0.00
6	1.27	0.00	7.00	0.00	n.a	0.00	7.00	0.00	8.65	0.00	7.00	0.00
8	12.62	0.00	6.00	0.00	n.a	0.00	6.00	0.00	9.52	0.00	6.00	0.00
10	0.56	0.44	5.00	4.36	n.a	0.00	5.00	0.00	3.53	0.00	5.00	0.00
12	2.11	0.00	4.00	0.00	3.87	0.00	4.00	0.00	0.89	0.10	4.00	0.80
14	0.70	0.30	3.00	1.80	9.96	0.00	3.00	0.00	2.68	0.00	3.00	0.00
16	0.49	0.49	2.00	2.03	1.93	0.00	2.00	0.00	1.03	0.00	2.00	0.00
18	11.12	0.00	1.00	0.00	n.a	0.00	1.00	0.00	n.a	0.00	1.00	0.00
20	9.37	0.00	0.00	0.00	n.a	0.00	0.00	0.00	n.a	0.00	0.00	0.00
22	11.28	0.00	0.00	0.00	10.91	0.00	0.00	0.00	5.16	0.00	0.00	0.00
24	7.35	0.00	0.00	0.00	11.04	0.00	0.00	0.00	2.74	0.00	0.00	0.00
26	11.40	0.00	0.00	0.00	7.73	0.00	0.00	0.00	5.31	0.00	0.00	0.00
28	8.88	0.00	0.00	0.00	n.a	0.00	0.00	0.00	n.a	0.00	0.00	0.00
30	9.81	0.00	0.00	0.00	n.a	0.00	0.00	0.00	n.a	0.00	0.00	0.00
Total Index				8.19				8.54				0.80

The determination of the Liquefaction Potential Index (LPI) ends the analysis of liquefaction potential in the Jogja-Solo Toll Road section located in Ngawen, Karangnongko, Kebonarum, and Jogonalan Sub-District. There is a difference in the number of liquefied boreholes compared to other adjacent research locations. Research by [31] analyzed the liquefaction potential from the east side of Ngawen to the Karanganom District, with 9 out of 10 boreholes indicating liquefaction potential. The research location shares this study's geological conditions: the Merapi Volcanic Rock (Qvm) [32]. Although the influence of fine grains is not explained in that study, the results of liquefaction potential analysis can differ under similar geological conditions. Several factors can contribute to these differences, such as lower SPT showed as soft soil site class (SE) or higher estimated PGA. The mentioned research estimated PGA based on Next Generation Attenuation (NGA)-WEST Campbell & Bozorgnia [33], considered by the amplification factor (F_{PGA}) based on [29]. The results differ significantly from this research, reaching 0.46 g – 0.57 g. Such a PGA seems to have a higher return period than the estimated PGA in this research. If this research applies the same method to estimate PGA, the results are 0.57 g – 0.67 g. This PGA value indicates liquefaction potential in 11 out of 21 boreholes, resulting in a 47% decrease in the factor of safety.

5. CONCLUSIONS

The Jogja-Solo Toll Road, a national strategic project crucial for economic and tourism growth, is situated in a seismic-prone area, forming the basis for this research's liquefaction potential analysis. The study results indicate that 3 out of 21 boreholes in Section 1.2, STA 22+475 – STA 29+000, exhibit liquefaction potential with an FS < 1. These three boreholes—BH-60 and BH-67, with a high liquefaction potential index, and BH-156, with a low liquefaction potential index—successfully passed the identification stage based on gradation criteria and soil properties. This initial stage ensures that layers with FS < 1 display grain behavior susceptible to liquefaction during an earthquake, with BH-67 identified as having the highest fine content compared to the other two boreholes. Alternative approaches, such as numerical methods, could be used to analyze this condition further, considering the influence of confining stress and initial void ratio in evaluating liquefaction potential. Moreover, locations identified with liquefaction potential necessitate follow-up actions involving mitigation measures such as installing stone columns or soil replacement, as layers with liquefaction potential vary in depth. Implementing mitigation structures, guided by a comprehensive liquefaction potential analysis, is a sustainable contribution to natural disaster management in

construction, particularly in areas with high seismic vulnerability.

6. ACKNOWLEDGMENTS

The authors sincerely thank the Directorate General of Highways, the Ministry of Public Works and Housing, and PT Jogjasolo Marga Makmur.

7. REFERENCES

[1] Murjaya J., Pramumijoyo S., Karnawati D., Meilano I., Supendi P., Ahadi S., Marliyani G. I., Syukur F., Sianipar D. S., and Krisno A., Earthquake Risk Assessment of the Opak and Merapi-Merbabu Active Faults to Support Mitigation Program in Yogyakarta Province and Its Vicinity, In IOP Conference Series: Earth and Environmental Science, vol. 851, 012001, 2021, pp. 1-11.

[2] Partono W., Nazir R., Kistiani F., and Sari U. C., Seismic Microzonation of Yogyakarta Province Based on 2019 Risk-Targeted Maximum Considered Earthquake, In International Conference on Rehabilitation and Maintenance in Civil Engineering, Singapore: Springer Nature Singapore, 2021, pp. 489-497.

[3] Adam J. A. N., Widjajanti N., and Pratama C., Estimation of Slip Rate and the Opak Fault Geometry Based on GNSS Measurement, In IOP Conference Series: Earth and Environmental Science, vol. 1039, 012058, 2022, pp. 1-8.

[4] Rahman M.A., Fathani T.F., Rifa'i A., and Hidayat M.S., Analisis Tingkat Potensi Likuifaksi Di Kawasan Underpass Yogyakarta International Airport, Jurnal Rekayasa Sipil 16, no. 2, 2020, pp. 91-104.

[5] Lakkimsetti B., and Latha G.M., Role of Grain Size and Shape on Undrained Monotonic Shear, Liquefaction, and Post-Liquefaction Behaviour of Granular Ensembles, Soil Dynamics and Earthquake Engineering, vol 173, 108086, 2023, pp. 1-23.

[6] Sauri S., Rifa'i A., and Hardiyatmo H. C., Liquefaction Vulnerability Analysis using N-SPT Value and Grain Size Analysis on Gumbasa Irrigation Canal in the Post-Disaster Petobo Area, Sulawesi, In IOP Conference Series: Earth and Environmental Science, vol. 930, 012081, 2021, pp. 1-11.

[7] Rahayu W., Nurizkatilah, and Bahsan E., Analysis of Liquefaction Potential in Lolu Village, Palu using SPT Method and Laboratory Test of Grain Size Distribution, In IOP Conference Series: Earth and Environmental Science, vol. 622, 012016, 2021, pp. 1-8.

[8] Liu W., Ishii K., and Kamao S., Effect of Fines Content on Liquefaction Characteristics, GEOMATE Journal 20, no. 82, 2021, pp. 40-45.

[9] Manzanal D., Bertelli S., Lopez-Querol S., Rossetto T., and Mira P., Influence of Fines Content on Liquefaction from a Critical State Framework: the Christchurch Earthquake Case Study, Bulletin of Engineering Geology and the Environment, vol. 80, 2021, pp. 4871-4889.

[10] Wang W., Some Findings in Soil Liquefaction, Water Conservancy and Hydroelectric Power Scientific Research Institute, Bejing, China, 1979, pp. 1-17.

[11] Seed H.B., and Idris I.M., Ground Motions and Soil Liquefaction During Earthquakes, Earthquake engineering research insititue, 1982, pp. 1-134.

[12] Yao K., Rong Y., Yao Z, Shi C., Yang C., Chen L., Zhang B., and Jiang H., Effect of Water Level on Dynamic Compaction in Silty Ground of Yellow River Alluvial Plain, Arabian Journal of Geosciences, vol. 15, 126, 2022, pp. 1-16.

[13] Jogjasolo Marga Makmur Corporation, Soil Investigation Jogja – Solo Toll Road, 2022, pp. 1-17.

[14] Nu, Nguyen Thi, Nguyen Thanh Duong, and Bui Truong Son, Assessment of Soil Liquefaction Potential Based on SPT Values at Some Ground Profiles in the North Central Coast of Vietnam, Iraqi Journal of Science, Vol. 62, No. 7, 2021, pp. 2222-2238.

[15] Tsuchida H., Prediction and Countermeasure Against the Liquefaction in Sand Deposits, In Abstract of the Seminar in the Port and Harbor Research Institute, 1970, pp. 3.1-3.33.

[16] USGS, M6.3 Java Earthquake of May 26 2006, Accessed June 20 2023, https://earthquake.usgs.gov/product/poster/20060526/us/1461770047809/poster.pdf

[17] Kanno T., Narita A., Morikawa N., Fujiwara H., and Fukushima Y., A New Attenuation Relation for Strong Ground Motion in Japan Based on Recorded Data, Bulletin of the Seismological Society of America, vol. 96, no. 3, 2006, pp. 879-897.

[18] Taruna R.M., and Setiadi T.A.P., Penentuan Rumus Percepatan Tanah akibat Gempabumi di Kota Mataram Menggunakan Metode Euclidean Distance, JST (Jurnal Sains dan Teknologi), vol. 9, no. 1, 2020, pp. 20-29.

[19] Muktaf H.A., Wiyono., and Tampubolon B. D., New Approach for Developing Correlation of NSPT and Shear-Wave Velocity (Vs): Bantul Case Study, Indonesian Journal on Geoscience, vol. 9, no. 3, 2022, pp. 395-413.

[20] Idriss I. M., and Boulanger R. W., Soil Liquefaction During Earthquakes, Earthquake Engineering Research Institute, 2008, pp. 1-120

[21] Alexandr G., and Chi T.N., Liquefaction Possibility of Soil Layers During Earthquake In Hanoi, GEOMATE Journal 13, no. 39, 2017, pp.

148–155.
[22] Boulanger R. W., and Idriss I.M., CPT and SPT Based Liquefaction Triggering Procedures, Centre for Geotechnical Modelling, Report No. UCD/CGM-14/01, 2014, pp. 1-134.
[23] Seed H. B., and Idriss I.M., Simplified Procedure for Evaluating Soil Liquefaction Potential, Journal of the Soil Mechanics and Foundations division, vol. 97, no. 9, 1971, pp. 1249-1273.
[24] Hakam A., Febriansyah D., Adji B.M., Junaidi, Liquefaction Mapping Procedure Development: Density and Mean Grain Size Formulations, GEOMATE Journal 18, no. 70, 2020, pp. 155-161.
[25] Iwasaki T., Tokida K.I., Tatsuoka F., Watanabe S., Yasuda S., and Sato H., Microzonation for Soil Liquefaction Potential using Simplified Methods, In Proceedings of the 3rd International Conference on Microzonation, Seattle, vol. 3, no. 2, 1982, pp. 1310-1330.
[26] Sonmez H., Modification of the Liquefaction Potential Index and Liquefaction Susceptibility Mapping for a Liquefaction Susceptibility Mapping for a Liquefaction-Prone Area (Inegol, Turkey), Environmental Geology, 44, 2003, pp. 862-871.
[27] Ishihara K., Stability of Natural Deposits during Earthquakes, In Proceedings of the 11th International Conference on Soil Mechanics and Foundation Engineering, San Francisco, A. A. Balkema, Rotterdam, 1985, pp. 321-376.
[28] Ashadi A.L., Harmoko U., Yuliyanto G., and Kaka S.I., Probabilistic Seismic - Hazard Analysis for Central Java Province, Indonesia, Bulletin of the Seismological Society of America 105, no. 3, 2015, pp. 1711-1720.
[29] National Standardization Agency, SNI 1726:2019 Guidelines for Earthquake Resistance Planning for Structures of Buildings and Non-Buildings, Jakarta, Indonesia, 2019, pp. 1-250.
[30]Pawirodikromo W., The Estimated PGA Map of the Mw6.4 2006 Yogyakarta Indonesia Earthquake, Constructed from the Modified Mercalli Intensity IMM, Bulletin of the New Zealand Society for Earthquake Engineering, vol. 51, no. 2, 2018, pp. 92-104.
[31] Yulianisa Y., Hardiyatmo H.C., and Faris F., The Effect of Opak Fault on Liquefaction Potential at Toll Road Construction in Klaten Regency, Central Java, In IOP Conference Series: Earth and Environmental Science, vol. 1203, 012030, 2023, pp. 1-9.
[32] Surono B. T., and Sudarno I., Geological Map of The Surakarta – Giritontro Quadrangle, Jawa, scale 1:100,000, Geological Research and Development Centre, Bandung, 1992, pp.1.
[33] Campbell K., W., and Bozorgnia Y., NGA-West2 Ground Motion Model for The Average Horizontal Components of PGA, PGV, and 5% Damped Linear Acceleration Response Spectra, Earthquake Spectra 30, no. 3, 2014, pp.1087-1115.